Vital Annex: International Journal of Novel Research in Advanced Sciences
ISSN: 2751-756X
Volume 04 Number 09 (2025)
https://innosci.org/IJNRAS

Article

Appraisal of An Oil Field's Air Quality Using Geomatics Techniques and Field Survey

Khaldoon T. Falih[1] , Ahmed Salman Hasana[2]

1. Civil Techniques Department, Nasiriyah Technical Institute, Southern Technical University, Baghdad Street, Nasiriyah 64001, Iraq
2. Civil Techniques Department, Nasiriyah Technical Institute, Southern Technical University, Baghdad Street, Nasiriyah 64001, Iraq

* Correspondence: khaldoon.ta;jb@stu.edu.iq

Abstract: In countries that produce petroleum, waste streams and petroleum hydrocarbons have deteriorated host towns, contaminated the environment, and negatively impacted human health and socioeconomics. Due to the difficulty of obtaining large volumes of samples and the high cost of laboratory research to evaluate element concentrations, it has been difficult to determine the level of contamination from a limited number of samples, especially at oil sites. Finding hotspots of contaminated air, developing geospatial risk maps of petroleum industry pollution, and determining which locations need urgent attention because they are most affected by petroleum activities are the goals of the project. Total suspended particulate matter (TSP), PM10, carbon monoxide (CO), carbon dioxide (CO2), hydrogen sulphide (H2S), sulphur dioxide (SO2), nitrogen dioxide (NO2), and hydrocarbon content were measured once a month for six months at 14 locations in the Al-Gharraf oil field. The threshold values for some components, such PM10 and H2S, were 0.1 mg/m3 and 0.5 ppm, respectively, and were exceeded at many locations, even if the bulk of the concentrations were under the set level. Several strategies and tactics were employed to accomplish the aforementioned goals, one of which was the Inverse Distance Weighting (IDW) methodology combined with GIS (to create geographical maps of the observed values).The distribution of the several environmental characteristics throughout the oil field was accurately and efficiently mapped using the IDW technique. Every month, the analysis is conducted and contrasted with the limit value. For the oil industry, this study has produced a valuable database that should be utilised consistently to track ecosystem health

Citation: Falih, K. T & . Hasana, A. S. Appraisal of An Oil Field's Air Quality Using Geomatics Techniques and Field Survey. Vital Annex: International Journal of Novel Research in Advanced Sciences 2025, 4(9), 445-453

Received: 10th Aug 2025
Revised: 16th Sep 2025
Accepted: 24th Oct 2025
Published: 28th Nov 2025

Keywords: petroleum hydrocarbon, geographic information system (GIS), concentrations; inverse distance weighting (IDW), air contamination, oil field.

1. Introduction

The petroleum hydrocarbon contamination of ecosystems is a significant global environmental issue that has garnered public attention in recent decades. One of the primary factors contributing to the release of hydrocarbons through agricultural or industrial products is human activities. Although petroleum is a primary energy source that contributes to the economic and social developments of a nation, it has become one of the most significant organic pollutants. This is due to the crude oil combustion emissions

to air, primary leakage of underground storage tanks and accidental spills during transportation and disposal [1]. The environmental pollution, adverse environmental and/or human health problems, negative impacts on the terrestrial ecosystems, detrimental impacts on the regional economy, socio-economic problems, and degradation of oil-producing host communities in these countries have been caused by the inadvertent discharges of petroleum hydrocarbons and chemical-derived waste streams resulting from petroleum exploration and production [2]. The unintended release of petroleum hydrocarbons into the environment results in several repercussions, including (i) atmospheric pollution resulting from natural gas flaring and venting, potentially exacerbating the global climate change; (ii) marine ecosystem pollution, likely leading to detrimental effects on wildlife and adverse consequences for tourism, fishing, and related industries; (iii) contamination of soil and regulated water sources (both surface and groundwater); (iv) socio-economic challenges and degradation of cultural heritage in affected oil-producing host communities; (v) land contamination, compromised food quality, and diminished agricultural output [3].

Because geographic information systems (GIS) seamlessly combine geographical and temporal variables, they are proving to be indispensable tools for holistic air quality evaluation [4]. This technology provides scientists and resource managers with a strong platform for analysis and simulation, aiding in the visualization of complex linkages [5]. GIS software is no longer limited to managing and processing geographic data. These days, it includes the administration and processing of many kinds of geographic data [6]. Geographic information systems (GIS) have been demonstrated to be invaluable tools for comprehensive air quality evaluation since they effectively incorporate spatial and temporal variables [7].

The investigation aims to: (i) appraise and characterise the petroleum contamination hotspot within the oil field; (ii) Visualise spatial and temporal fluctuations of these characteristics using GIS-based interpolation and overlay analysis methods; and (iii) assess which areas require immediate care since they are most impacted by petroleum activity. Furthermore, this study demonstrates the accuracy of the (IDW) approach with a small sample size, which presents a problem for many pollution management-focused institutions because they must collect more samples and invest more time.

2. Materials and Methods

This research focuses on the Garraf oil field in southern Iraq, located approximately 31° 38′ 15″ to 31° 40′ 53″ N and 45° 51′ 20″ to 46° 2′ 54″ E. Fourteen stations were chosen at the Al-Garraf oil field in the Thi-Qar governorate to monitor gaseous emissions seasonally from March 2022 to August 2022 Figure . The selected stations continue to monitor the ambient air quality and gaseous emissions from nearby industrial facilities. In this study, the following gases were measured: total suspended particulate (TSP), PM10, carbon monoxide (CO), carbon dioxide (CO2), hydrogen sulphide (H2S), sulphur dioxide (SO2), nitrogen dioxide (NO2), and hydrocarbon content. CO2, SO2, NO2, and hydrocarbon content concentrations are measured using the portable detection instrument of Drager Chip-Measurement System, Germany, while CO and H2S concentrations are measured using the portable detection instrument of RK1 Gas Monitoring Eagle II, United States. Lastly, TSP and PM10 were measured using Clarity's Sensing's Particulate Monitor (Table 1).

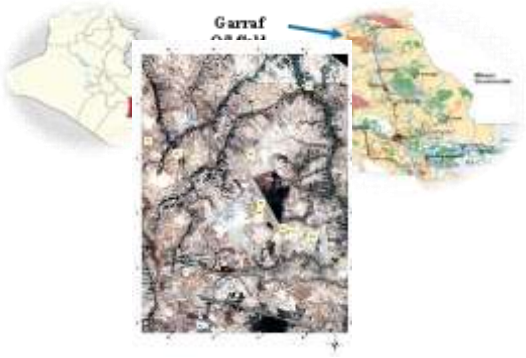

Figure 1. Geographic location and distribution of air quality sampling sites in the Garraf oil field

Table 1. Details of air sampling in the Al-Garraf oil field.

Location ID	GPS Coordinate	
	Longitude	Latitude
A-1	31°47′54.58″ N	46°00′57.32″ E
A-2	31°47′36.40″ N	46°03′32.70″ E
A-3	31°47′30.10″ N	46°02′08.50″ E
A-4	31°49′09.20″ N	46°04′59.40″ E
A-5	31°46′13.60″ N	46°03′41.50″ E
A-6	31°46′16.90″ N	46°03′46.20″ E
A-7	31°46′29.70″ N	46°03′47.40″ E
A-8	31°45′56.50″ N	46°04′19.80″ E
A-9	31°45′10.50″ N	46°05′53.40″ E
A-10	31°45′44.60″ N	46°05′04.20″ E
A-12	31°45'51.97" N	46°04'35.18" E
A-13	31°46′25.20″ N	46°03′50.80″ E
A-14	31°46′19.70″ N	46°03′37.30″ E

ArcGIS, developed by ESRI, was used extensively for data entry, analysis, and mapping. Thi-Qar Oil Company (TOC) provided the basic map depicting the Garraf oilfield's borders. The raster data from the base map was transformed to vector data, and the sampling spots' coordinates were captured using a GPS. ArcCatalog was used to construct an air quality database for all observed stations, while ArcGIS 10.7 enhancements aided in analysis, interpolation, and mapping.

The IDW technique, which was applied using ArcGIS 10.3's Extension for Spatial Analyst, was based on laboratory experiments performed at 14 different places along the oil field. The extra data collected at the measurement stations for each parameter was used to create the interpolated cells used in the air site construction.

3. Results

Monitoring and Spatial Interpolation of Air Contamination

Contamination in the air comes from both natural and human sources. Automobiles, power plants, and industrial activities are some of the main sources of air pollution that are caused by humans. Compared to other industries, oil industrial activities, such as power plants and oil refineries, produce a high number of emissions of smoke, solid particulates, and toxic gases [8]. The presence of these industries within the city limits or urban areas, such as the Garraf oil field, will make them more hazardous. The oil industry is regarded as a significant contributor to air pollution, and the volumes of the pollutants that are released into the air by these industries are estimated to be in the millions of tons per year [9], [10]. The following gases were measured: total suspended particulate (TSP), PM_{10}, carbon monoxide (CO), carbon dioxide (CO_2), hydrogen Sulphide (H_2S), sulphur dioxide (SO_2), nitrogen dioxide (NO_2), and hydrocarbon content. Furthermore, the concentrations of these elements will be displayed by stations and months during the duration of the study, in addition to the average concentrations of these components, as depicted in Figure 2. The results of assessing the quality of the air within the Al-Garraf oil field, and chemical element measurements to identify hot spots and those most affected by pollutants to achieve the first objective of the study are also shown [11]. The mean concentrations recorded over six months, from March to August 2022, are presented in Table 2. Utilizing the requisite apparatus and instruments, the values were acquired before undergoing the laboratory analysis.

Table 2 . Results of parameters measured on air quality samples from the Al-Garraf oil field.

	Units	Sample ID													Measuring Equipment	Max. Allowable Iraqi National Limits
		A-1	A-2	A-3	A-4	A-5	A-6	A-7	A-8	A-9	A-10	A-12	A-13	A-14	A-15	
TS	mg/	0.1	0.2	0.1	0.1	0.1	0.1	0.1	0.1	0.1	0.1	0.2	0.1	0.1	0.1	
P	m³	90	20	94	85	82	81	95	95	81	91	25	86	79	78	0.350
PM	mg/	0.1	0.0											0.0	0.0	
10	m³	07	9											3	72	0.100
Temperature	°C	39	4											4	40	
CO	ppm	1.7	2.											.1	2.1	35
		51	7											7	88	
CO_2	%	0.4	0.											.4	0.4	2.5%
		81	7											5	91	
H_2S	ppm	0.1	0.											.2	0.5	0.5
		50	8											0	08	
SO_2	ppm	0.0	0.											.0	0.1	0.15
		64	5											1	00	
NO	ppm	0.0	0.											.0	0.0	0.1
2		90	7											6	82	
Hydrocarbon	ppm	0.1	0.											.1	0.1	0.24
		02	1											0	08	

Gases Detector (Microreactor)

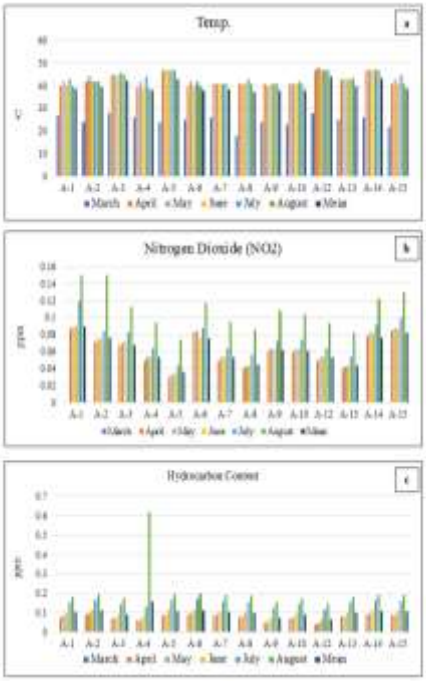

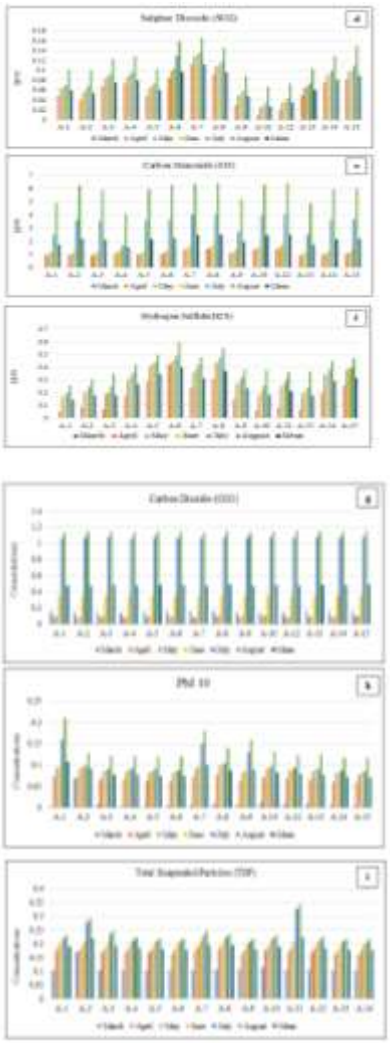

Figure 2. Monthly concentrations of (a) Temperature, (b) NO_2, (c) Hydrocarbon Content, (d) SO_2, (e) CO, f-H_2S, g- CO_2, h-PM_{10}, i- TSP,) at Al-Garraf oil field

An increase in concentrations can be seen for August, as seen in Figure 3. This figure encompasses the components that were used to examine the distribution of station concentrations over the months. As a result of the investigation into this subject, it was discovered that the number of production activities rose during this month in comparison to the subsequent months. The mean of Nitrogen Dioxide (NO_2) levels in the 14 sampling locations for 6 months ranged from a minimum of 0.036 ppm in location (A-5) to a maximum of 0.09 ppm in location (A-1). The results did not exceed the maximum acceptable Iraqi National Limit of NO_2 (0.1 ppm) Figure 4.3(b) illustrates all recorded data [12].

The mean of hydrocarbon content levels in the 14 sampling locations for 6 months ranged from a minimum of 0.068 ppm in location (A-12) to a maximum of 0.16 ppm in location (A-1). The results did not exceed the maximum acceptable Iraqi National Limits of Hydrocarbon Content (0.24 ppm), and Figure 4.3(c) illustrates all the recorded data. The mean of Sulphur Dioxide (SO_2) levels in the 14 sampling locations for 6 months ranged from a minimum of 0.029 ppm in location (A-10) to a maximum of 0.154 ppm in location (A-8). The results of the maximum acceptable Iraqi National Limits of SO_2 (0.15 ppm) in locations (A-7, A-8), can be seen in Figure 3(d).

The mean of Carbon Monoxide (CO) levels in the 14 sampling locations for 6 months ranged from a minimum of 1.556 mg/m^3 in location (A-4) to a maximum of 2.511 mg /m^3 in location (A-8). The results did not exceed the maximum acceptable Iraqi National Limits of PM_{10} (35 ppm), and Figure 4.3(e) illustrates all recorded data. Additionally, the mean of hydrogen sulphide (H_2S) levels in the 14 sampling locations for 6 months ranged from a

minimum of 0.15 ppm in location (A-1) to a maximum of 0.508 ppm in location (A-14). The results exceed the maximum acceptable Iraqi National Limits of H_2S (0.5 ppm) in location (A6 – A14), and Figure 3(f) illustrates all the recorded data

The mean of carbon dioxide (CO_2) levels in the 14 sampling locations for 6 months ranged from a minimum of 0.475 % in location (A-4) to a maximum of 0.493 % in location (A-8). The results did not exceed the maximum acceptable Iraqi National Limit of CO_2 (2.5%). Figure 4.3(g) illustrates all of the recorded data. The mean of Particulate matter 10 (PM_{10}) levels in the 14 sampling locations for 6 months ranged from a minimum of 0.072 mg/m3 in location (A-14) to a maximum of 0.107 mg /m^3 in location (A-1). The results exceed the maximum acceptable Iraqi National Limits of PM_{10} (0.100 mg /m^3) in location (A-1, A-7). Figure 4.3(h) illustrates all of the recorded data. Finally, the mean of TSP levels in the 14 sampling locations for 6 months ranged from a minimum of 0.178 mg/m^3 in location (A-14) to a maximum of 0.225 mg /m^3 in location (A-11). The results did not exceed the maximum acceptable Iraqi National Limits of TSP (0.350 mg /m^3), and Figure 3(i) shows all the TSP data [13]. Stations (A-1) and (A-8) were the stations that were most affected. This is because Station (A-1) is the region where waste from oil activities is disposed of, which is the source of pollution. On the other hand, Station (A-8) is a gathering station for many of the fluids utilized in extraction activities. As a result, pollutants are emitted from it, and it is located near the flare of the oil tower.

GIS is employed as a vehicle for the spatial-temporal data analysis or for creating a joint GIS database environment that drives stand-alone modelling tools. This creates a huge problem because air data is usually a mess because there is a high degree of correlation among many pollutants [14]. The outcomes of these techniques were almost as diverse as the techniques themselves, showing once again that the complex phenomenon of air quality management calls for methods and tools that are not only sensitive but also capable of such high degrees of accuracy and probability. Additionally, numerous studies have been conducted regarding the GIS component of the spatio-temporal analysis of urban air quality [15].

The GIS technology development opens up the possibility of applying spatial numerical interpolation everywhere. Primarily Original Kriging, Spline (Cubic Spline Interpolation), and IDW are the most employed interpolation methods [16]. Among these three approaches, IDW is very convenient to use, with a data integration rate higher than 75% through spatial interpolation, hence resulting in the prediction accuracy of normal data that can be improved by applying analytical tools for data exploration [17]. This was illustrated through numerous experiments performed within the research, which revealed that the IDW method yielded the most accurate and optimal map. All measured atmospheric components were subjected to the IDW method, as illustrated in Figure 3. The risk maps below are presented as a result of the second objective of this study [18].

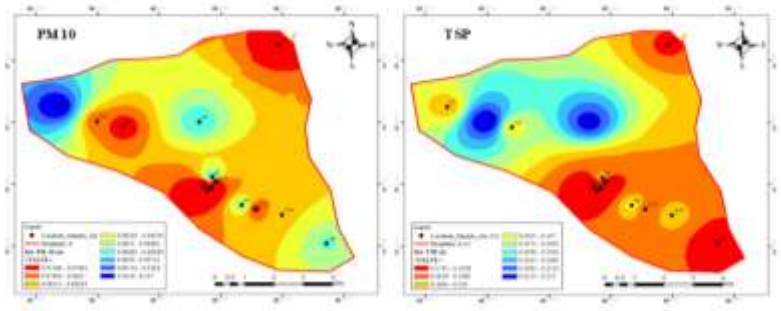

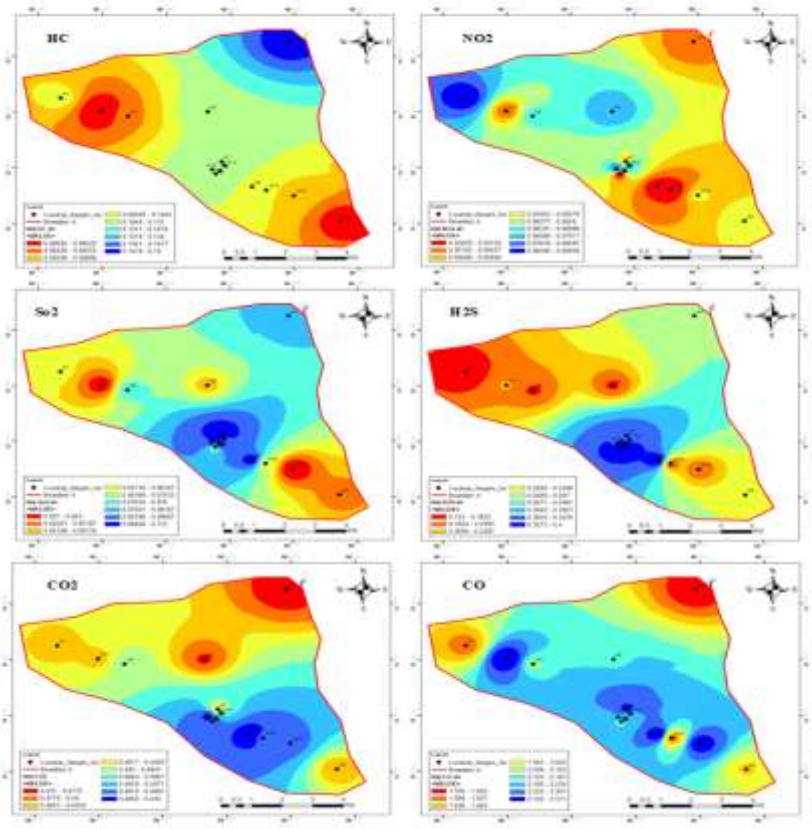

Figure 3. Spatial distribution of physico-chemical parameters (air) at the Al-Garraf oil field

From Figure 4, the highest amounts of nitrogen dioxide (NO_2) (0.0815–0.09 ppm) are seen in the vicinity of station A1, which is consistent with combustion processes like flaring or vehicle emissions. The middle zone exhibits moderate concentrations, while the eastern and southwestern zones, particularly those close to stations A4 and A9, show the lowest NO_2 values (0.0385–0.0471 ppm). The spatial pattern indicates that NO_2 is concentrated near areas of operational activity. Hydrocarbons (HC), mostly from oil operations and incomplete combustion, peak in the northeast around station A4 (0.146–0.16 ppm). Given that the majority of other stations displayed moderate levels, this is a noteworthy oddity. The regions near stations A1, A11, and A9, where the lowest HC concentrations (0.0682–0.0835 ppm) were found, had less influence [19]. The elevated HC around A4 may indicate fugitive emissions or leaks from nearby pipelines or processing plants. The higher concentrations (0.0976–0.112 ppm) near station A5 on the SO_2 map indicate that the emissions of sulphur dioxide (SO_2) are caused by burning fossil fuels or the release of sulfur-bearing gas. On the other hand, the northeast and southern periphery close to stations A4 and A9 exhibit lower amounts (0.0274–0.0414 ppm). The trend shows that the operational zone has the highest concentration of industrial gas emissions [20].

Given that the majority of other stations displayed moderate levels, this is a noteworthy oddity. The regions near stations A1, A11, and A9, where the lowest HC concentrations (0.0682–0.0835 ppm) were found, had less influence. The elevated HC around A4 may indicate fugitive emissions or leaks from nearby pipelines or processing plants. The higher concentrations (0.0976–0.112 ppm) near station A5 on the SO_2 map indicate that the emissions of sulphur dioxide (SO_2) are caused by burning fossil fuels or the release of sulfur-bearing gas [21]. On the other hand, the northeast and southern periphery close to stations A4 and A9 exhibit lower amounts (0.0274–0.0414 ppm). The trend shows that the operational zone has the highest concentration of industrial gas emissions.These hotspots are crucial for mitigation since H_2S is a major indicator of sour gas leaks and presents a health risk at high levels [22]. The range of concentrations in the CO_2 distribution is somewhat limited. The central-east area next to station A5 had the

highest values (0.491–0.493%), suggesting combustion processes and potential CO_2 emissions from machinery or flaring. The northeastern area close to station A4 has lower CO_2 readings (0.475–0.478%), indicating cleaner air there. Although small elevations may suggest localised anthropogenic sources, the spatial homogeneity reflects the well-mixed nature of CO_2 in the atmosphere [23].

The central-west zone has moderate to elevated PM_{10} levels, with a peak range of 0.102–0.107 mg/m³ close to station A1. This is probably caused by open waste burning, machinery movement, and dust from unpaved roads. Station A4 and other peripheral sites reported lower PM_{10} values (0.0723–0.0781 mg/m³), suggesting that the ambient air was cleaner further from the operations centre. Because of flaring and petroleum operations, TSP levels in the central zone, especially close to stations A2 and A3, peak between 0.2170-0.2247 mg/m³. Near station A4, the lowest TSP values (0.1782–0.1860 mg/m2) were recorded, indicating that less disturbed areas had lower levels of airborne dust and contaminants.

4. Conclusion

The major aim of this inquiry is the full assessment of the air quality in the entire Garraf oil field from March 2022 up to and including August. Through suitable sampling and laboratory analysis, we were able to estimate the physicochemical parameters such as total suspended particulate (TSP), PM10, carbon monoxide (CO), carbon dioxide (CO_2), hydrogen sulfide (H2S), sulphur dioxide (SO_2), nitrogen dioxide (NO_2), and hydrocarbon content. After monitoring the concentrations of these components over a six-month period, the findings were compared to the acceptable limits, and the chemically polluted stations were determined. Using GIS and inverse distance-weighted interpolation (IDW), the temporal-spatial distribution of these contaminants was examined. The resulting chemical-physical pollution maps demonstrate that the most significant potential future source of pollution in the study area is the epicentre of oil activity, particularly the vicinity of the oil wells. There are several potentially harmful indications in the air around this location. In order to improve air quality, satisfy Iraqi standards and regulatory requirements, and safeguard the environment and public health, proactive methods like pre-treatment and air filtering are crucial.

REFERENCES

[1] S. Adipah, "Introduction of petroleum hydrocarbons contaminants and its human effects," Journal of Environmental Science and Public Health, vol. 3, no. 1, 2018.

[2] Arslan, "Treatability of a simulated disperse dye-bath by ferrous iron coagulation, ozonation, and ferrous iron-catalyzed ozonation," Journal of Hazardous Materials, vol. 85, no. 3, pp. 229–241, 2001.

[3] L. Bai, C. Li, C. W. Yu, and Z. He, "Air pollution and health risk assessment in northeastern China: A case study of Jilin Province," Indoor and Built Environment, vol. 30, no. 10, pp. 1857–1874, 2021.

[4] M. M. Barbooti, A. S. Hamadi, A. Abdul-Razzaq, and J. Hussain, "Environmental site assessment of Al-Daura refinery—Evaluation of soil pollution with petroleum products," Eng. & Tech. Journal, vol. 28, no. 20, 2010. [Online]. Available: www.pdffactory.com

[5] M. S. Boori et al., "Natural and environmental vulnerability analysis through remote sensing and GIS techniques: A case study of Indigirka River Basin, Eastern Siberia, Russia," in Earth Resources and Environmental Remote Sensing/GIS Applications VII, SPIE, 2016, p. 100050U.

[6] S. Chattopadhyay, S. Gupta, and R. N. Saha, "Spatial and temporal variation of urban air quality: A GIS approach," Journal of Environmental Protection, vol. 1, no. 3, pp. 264–277, 2010.

[7] K. Chen et al., "Risk assessment of nitrate groundwater contamination using GIS-based machine learning methods: A case study in the Northern Anhui Plain, China," Journal of Contaminant Hydrology, vol. 261, p. 104300, 2024. [Online]. Available: https://linkinghub.elsevier.com/retrieve/pii/S0169772224000044

[8] J. A. M. Demattê et al., "The Brazilian Soil Spectral Service (BraSpecS): A user-friendly system for global soil spectra communication," Remote Sensing, vol. 14, no. 3, 2022.
[9] D. Zhao et al., "GIS-based urban rainfall-runoff modeling using an automatic catchment-discretization approach: A case study in Macau," Environmental Earth Sciences, vol. 59, no. 2, pp. 465–472, 2009.
[10] B. Enkhtur, N. Hamm, and I. A. Stein, "Geostatistical modelling and mapping of air pollution," University of Twente, 2013.
[11] E. Ghaly and D. Dave, "Remediation technologies for marine oil spills: A critical review and comparative analysis," American Journal of Environmental Sciences, 2011.
[12] Lenart-Boro and P. Boro, "The effect of industrial heavy metal pollution on microbial abundance and diversity in soils — A review," in Environmental Risk Assessment of Soil Contamination, InTech, 2014.
[13] J. Li and A. D. Heap, "A review of comparative studies of spatial interpolation methods in environmental sciences: Performance and impact factors," Ecological Informatics, vol. 6, no. 3–4, pp. 228–241, 2011.
[14] J. Maantay, "Asthma and air pollution in the Bronx: Methodological and data considerations in using GIS for environmental justice and health research," Health and Place, vol. 13, no. 1, pp. 32–56, 2007.
[15] L. Matejicek, "Spatial modelling of air pollution in urban areas with GIS: A case study on integrated database development," Advances in Geosciences, vol. 4, pp. 63–68, 2005.
[16] S. Mtetwa, S. Kusangaya, and C. F. Schutte, "The application of geographic information systems (GIS) in the analysis of nutrient loadings from an agro-rural catchment," Water SA, vol. 29, no. 2, pp. 189–193, 2003.
[17] O. Oke and K. Ogedengbe, "Mapping of river water quality using inverse Ogun-Osun River Basin, Nigeria," Lanskap & Environment, vol. 7, no. 2, pp. 48–62, 2013.
[18] M. Onyegeme-Okerenta, O. L. West, and L. C. Chuku, "Concentration, dietary exposure and human health risk assessment of total petroleum and polycyclic aromatic hydrocarbons in seafood from coastal communities in Rivers State, Nigeria," Scientific African, vol. 16, 2022.
[19] V. O. Otitolaiye and G. M. Al-Harethiya, "Impacts of petroleum refinery emissions on the health and safety of local residents," Journal of Air Pollution and Health, vol. 7, no. 1, pp. 69–80, 2022. [Online]. Available: https://publish.kne-publishing.com/index.php/JAPH/article/view/8921
[20] S. Panigrahy, "Geospatial crime analytics: A GIS-based approach towards prediction of crime hotspots," Journal of LATEX Templates, 2021. [Online]. Available: https://engrxiv.org/preprint/view/1654
[21] N. H. Rahim et al., "Ecosystem services by urban forest (UF) towards climate change adaptation: A review," Polish Journal of Environmental Studies, vol. 33, no. 4, pp. 3503–3513, 2024.
[22] S. Song, "A GIS-based approach to spatio-temporal analysis of urban air quality in Chengdu Plain," ISPRS Archives, vol. 37, no. 2, pp. 1447–1450, 2008.
[23] G. Wattayakorn, "Petroleum pollution in the Gulf of Thailand: A historical review," Coastal Marine Science, vol. 35, pp. 234–245, 2012. [Online]. Available: https://www.researchgate.net/publication/235726311_Petroleum_pollution_in_the_Gulf_of_Thailand_A_historical_review